

High-Throughput Ellipsometric Characterization of Vapor-Deposited Indomethacin Glasses

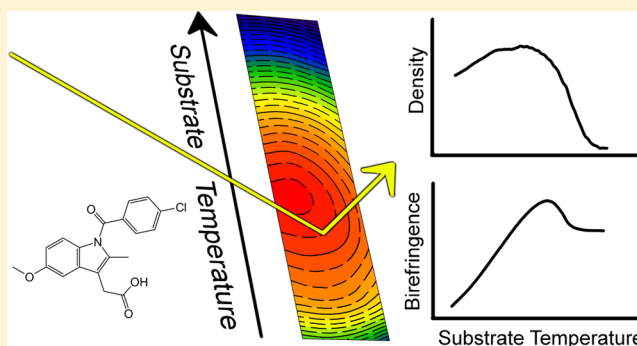
Shakeel S. Dalal,[†] Zahra Fakhraai,[‡] and M. D. Ediger^{*,†}

[†]Department of Chemistry, University of Wisconsin—Madison, Madison, Wisconsin 53706, United States

[‡]Department of Chemistry, University of Pennsylvania, Philadelphia, Pennsylvania 19104, United States

S Supporting Information

ABSTRACT: A method for the high-throughput preparation and characterization of vapor-deposited organic glasses is presented. Depositing directly onto a substrate with a large temperature gradient allows many different glasses to be prepared simultaneously. Ellipsometry is used to characterize these glasses, allowing the determination of density, birefringence, and kinetic stability as a function of substrate temperature. For indomethacin, a model glass former, materials up to 1.4% more dense than the liquid-cooled glass can be formed with a continuously tunable range of molecular orientations as determined by the birefringence. By comparing measurements of many properties, we observe three phenomenological temperature regimes. For substrate temperatures from $T_g + 11$ K to $T_g - 8$ K, equilibrium states are produced. Between $T_g - 8$ K and $T_g - 31$ K, the vapor-deposited materials have the macroscopic properties expected for the equilibrium supercooled liquid while showing local structural anisotropy. At lower substrate temperatures, the properties of the vapor-deposited glasses are strongly influenced by kinetic factors. Different macroscopic properties are no longer correlated with each other in this regime, allowing unusual combinations of properties.



INTRODUCTION

Organic glasses can be prepared by physical vapor deposition. Two recent developments have highlighted the important influence of the substrate temperature on the properties of glasses produced in this way. One development is in the field of organic electronics, where devices such as OLEDs often use vapor-deposited glasses as electron and hole transport layers. Yokoyama et al.^{1–6} and others^{7–16} have shown that vapor deposition can result in anisotropic films in which elongated molecules either tend to stand up or lie down, depending upon substrate temperature. For some systems, a factor of 10 change in the charge mobility was associated with changing the average molecular orientation in the glass.⁵ This result was attributed to overlap between the π systems of neighboring molecules being favored in some anisotropic packing arrangements. It has also been shown that the external quantum efficiency for OLEDs is higher when the transition dipoles of the emitter molecules lie in the plane of the device.¹⁷ For this case, device efficiency is increased for purely geometric reasons, because light is more efficiently coupled out of the device.

A second recent development concerns the kinetic stability of organic glasses prepared by vapor deposition. It has been shown that deposition onto substrates near $0.85 T_g$ can prepare glasses of organic molecules that, in addition to having extraordinary kinetic stability,^{18–21} are more dense^{22–24} and lower on the potential energy landscape^{25–28} than glasses

prepared by any other preparation route. While in principle these properties could be obtained by aging or slowly cooling the liquid, it is estimated that more than a thousand years would be required. Swallen et al.¹⁸ proposed that the efficient preparation of these “super-aged” materials is possible because the surfaces of organic glasses are highly mobile.²⁹ At substrate temperatures moderately below T_g , surface mobility allows molecules to sample various ways of packing before they become trapped by subsequent deposition. This partial equilibration allows more efficient packing than is achieved in an ordinary glass. Highly stable anisotropic glasses can be prepared in this regime, with molecular orientation depending upon substrate temperature.^{23,24} At much lower substrate temperatures, surface mobility is low relative to the deposition rate, resulting in poorly packed glasses.³⁰

These developments and others^{28,31} provide a clear incentive to understand at a fundamental level how the properties of vapor-deposited organic glasses depend upon the substrate temperature. For organic electronics, one may wish to use substrate temperature to manipulate molecular orientation in

Special Issue: Michael D. Fayer Festschrift

Received: May 21, 2013

Revised: July 12, 2013

Published: July 18, 2013

order to optimize charge mobility or charge injection.⁷ To advance our understanding of amorphous materials, one would like to know what deposition conditions produce glasses that are the closest to the equilibrium supercooled liquid.^{32–35} Unfortunately, systematically studying the glasses of even one molecule, produced at many different substrate temperatures, is generally quite time-consuming.

In this paper, we describe a high throughput characterization scheme for vapor-deposited organic glasses. Deposition occurs onto a substrate upon which we have imposed a temperature gradient, thus preparing a library of glasses from a single deposition. Subsequent ellipsometry measurements using a focused beam provide information about the density, birefringence, and kinetic stability of all these glasses, as described below. There are some precedents for this approach in the metal oxide field where temperature gradients have been used for sample preparation in conjunction with molecular beam epitaxy and pulsed laser deposition. In these cases, subsequent characterization was performed either by physically separating small portions of the samples or by probing small areas of the sample with techniques such as mechanical testing,³⁶ TEM,³⁷ SEM,³⁸ evanescent-probe microwave microscopy,³⁹ and surface X-ray diffraction.⁴⁰ While we are able to find some limited precedents for the use of temperature gradients to study thin films of organic materials,^{41–44} with a single exception,⁴⁵ these experiments did not involve vacuum deposition and the temperature gradient was used for sample analysis rather than sample preparation.

Here we use temperature gradients to prepare a library of vapor-deposited glasses of the model glass former indomethacin ($T_g = 309$ K at 1 K/min). The substrate temperatures surveyed span 120 K, with individual substrates having a temperature range of more than 100 K. By ellipsometrically mapping the substrate before and after the vapor-deposited glasses are transformed into the supercooled liquid, we can determine the density and birefringence at each substrate temperature; the birefringence is a probe of molecular orientation in the glass.^{2,24} During the thermal transformation, we also perform experiments analogous to conventional dilatometry to obtain the onset temperature that characterizes the kinetic stability of glasses deposited at 12 substrate temperatures.

By combining our results with published information about the properties of vapor-deposited indomethacin glasses, we find that there are three substrate temperature regimes. At temperatures as low as $T_g - 8$ K, all experimental observables indicate that vapor deposition prepares the equilibrium supercooled liquid at the deposition temperature. Between $T_g - 8$ K and $T_g - 31$ K, we are able to produce materials which have the macroscopic properties expected for the supercooled liquid while exhibiting indications of local packing anisotropy. Below $T_g - 31$ K, each experimental observable follows its own trend, indicative of a kinetically controlled regime. This low temperature regime produces materials with unusual combinations of properties not previously reported for liquid-cooled glasses.

EXPERIMENTAL METHODS

1. Sample Substrate. To enforce a temperature gradient across the sample substrate, silicon wafers were supported in a vacuum chamber by two fingers with independent temperature control, as shown in Figure 1. The substrate is coupled to the fingers via copper clamps that are held in place by stainless steel

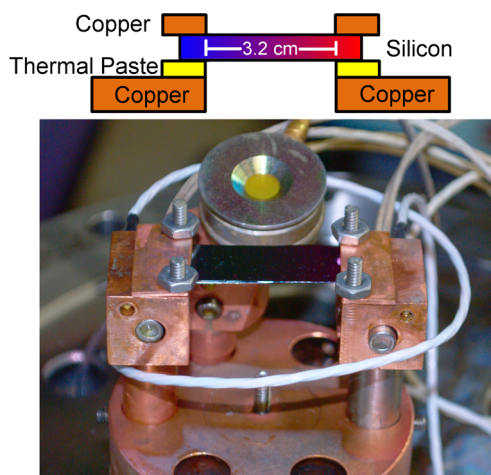


Figure 1. An image of the temperature gradient stage accompanying a schematic diagram. A silicon wafer bridges two fingers attached to a copper cold cup. Fingers are independently temperature controlled using cartridge heaters and platinum RTDs. The thermal conductance between the hot finger and the cold cup is reduced by using a low thermal conductivity material for the hot finger post. The quartz crystal microbalance used to monitor deposition rate is visible in the background.

nuts. Thermal contact is made between the finger and the silicon wafer with Apiezon N (M&I Materials Ltd.). The substrates were approximately 1.5 cm × 3.6 cm, with deposition occurring on the central 3.2 cm. The sample substrates were cut on the unpolished face of 500 μm silicon (100) wafers (Virginia Semiconductor) with a diamond scribe; the resulting silicon dust was removed from the substrates with nitrogen gas. Data from 24 of the 613 locations measured for these experiments were excluded due to the presence of silicon dust on the substrate at the measurement location.²³

Previously, Fakhraei et al. reported vapor-deposition of indomethacin onto a glass substrate with a temperature gradient.⁴⁵ A stainless steel bridge supported the substrate and enforced the temperature gradient. We have chosen not to utilize the stainless steel bridge in order to eliminate ambiguity about the true substrate temperature. The previous design relied on the large thermal conductance of stainless steel relative to glass, and inferred that the spatial dependence of the temperature in the bridge was the same in the glass. The higher thermal conductance of silicon does not allow this approach. By using only silicon to conduct heat between the two fingers, the temperature profile in the silicon wafer is dependent only on the known material properties of silicon and the end point temperatures. By ensuring that thermal contact occurs only at known locations, it is possible to calculate the temperature profile of the substrate by using internal calibration points, even when the thermal contact between the silicon and the copper clamps is imperfect. This procedure also eliminates the need to measure the temperature at every point on the sample using a pyrometer or thermocouple as in some previous experiments.

The relationship between substrate temperature and position, $T(y)$, is calculated by solving Fourier's Law:

$$q = -k[T(y)] \cdot A \cdot \frac{dT(y)}{dy} = -\frac{A}{y} \int_{T_{\text{cold}}}^{T_{\text{hot}}} k[T(y)] dT \quad (1)$$

Here, T_{hot} is the temperature at the hot end of the wafer, T_{cold} is the low temperature at the cold end of the wafer, y is the length

over which the gradient extends (3.2 cm), k is the thermal conductivity of silicon,⁴⁶ A is the cross-sectional area of the wafer, and q is the heat flow required to maintain the gradient. Equation 1 was numerically solved using Mathematica 8.0.⁴⁷

Because we are not able to achieve perfect thermal contact between the silicon wafer and the copper fingers in the presence of large heat flows, it is necessary to use internal calibration points to ensure temperature accuracy. T_{hot} is adjusted such that the data agrees with the density of the supercooled liquid at 305 K. T_{hot} is between 4 and 11 K below the RTD temperature, except for a single sample where the difference was 21 K. T_{cold} is adjusted such that the birefringence data agrees with those measured on samples with a single substrate temperature,²⁴ and is greater than the temperature of the RTD on the cold side by 0–9 K. The cross-sectional area of the silicon wafer is assumed to be constant. The contribution of indomethacin to the thermal conductivity of the sample can be disregarded, as it contributes a negligible amount to the cross-sectional area through which heat is being conducted and has low thermal conductivity in comparison to silicon.

II. Film Preparation. Films were deposited in an oil free vacuum chamber with a base pressure less than 10^{-7} Torr, as previously described.²³ When the chamber is at base pressure, the fingers are cooled. The independent heaters in the two fingers heat against the copper cold cup and are controlled by a Lakeshore 336 temperature controller. Once the deposition temperature has been established, crystalline indomethacin (>99% purity, Sigma-Aldrich) is heated in an alumina crucible 18 cm from the substrate, while a line-of-sight shield protects the substrate from deposition. After the rate of deposition is constant, as established by a quartz crystal microbalance (temperature controlled with a Lakeshore 340), the line-of-sight shield is lowered. The true rate of deposition is 0.2 nm/s \pm 10%, as determined by taking the maximum thickness of the sample (determined by ellipsometry) and dividing by the time of deposition. All samples used in these experiments were about 600 nm thick.

At the end of the deposition, the shield is replaced to its original position and the hot finger is cooled at 1 K/min until it reaches 305 K. (This is below the conventional glass transition temperature for indomethacin at a cooling rate of 1 K/min, determined to be 309 K.) The two fingers making up the temperature gradient holder are then brought to 285 K. The chamber is then vented with dry nitrogen gas, and the sample is immediately measured by ellipsometry. Approximately 40 min elapse from the end of deposition to the start of ellipsometry measurements.

III. Sample Analysis. The vapor-deposited indomethacin glasses are characterized using spectroscopic ellipsometry. Ellipsometry is a technique in which interference effects for carefully prepared polarized light are used to determine the thickness and index of refraction of thin film materials. The ellipsometer used here is a J. A. Woollam M-2000 spectroscopic ellipsometer with a wavelength range from 370 to 1000 nm, a continuously adjustable incident angle, and a focused spot size of approximately 0.6 mm \times 1.5 mm. A custom built temperature controlled translation stage was utilized; the stage holds substrates in place using a mild suction to ensure good thermal contact and consistent optical alignment. Samples can be reproducibly translated with positional precision of 2.5 μm on both the X and Y axis (manufacturer's specification). The temperature stage and ellipsometer were coordinated with LabView. The index of refraction of indomethacin is modeled

using the uniaxial anisotropic Cauchy model previously discussed, using only data from $\lambda = 500$ nm to $\lambda = 1000$ nm.²³ The Cauchy model has three parameters describing the wavelength dependence of the index of refraction in the normal dispersive regime, with an additional parameter added to allow wavelength-independent birefringence. The imaginary part of the index of refraction is fixed to zero. In modeling the data, the instrument bandwidth is fixed to 4.2 nm, the angular spread induced by focusing optics is 2°, and a parameter to account for a thickness gradient across the spot is typically <1%. The addition of surface roughness within an effective medium approximation does not improve the data fit, so we conclude there is no ellipsometrically detectable roughness.

The initial ellipsometric measurement of the sample is a mapped grid (see Figure 2) taken at 293 K at incident angles of

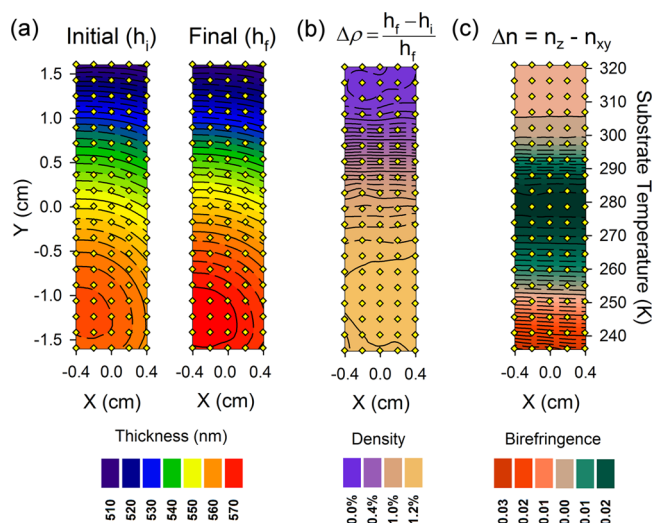


Figure 2. Ellipsometric characterization of vapor-deposited glasses of indomethacin, utilizing sample D for illustration. (a) The initial thickness of the sample (h_i) is measured at many locations on a grid pattern. After annealing, the same locations are remeasured to determine the final thickness h_f . (b) The density of as-deposited materials relative to the ordinary glass ($\Delta\rho$) can be determined by comparing the initial and final thicknesses. (c) The birefringence of the as-deposited material is also determined in the initial ellipsometric mapping of the sample. In contrast to the initial and final thickness, both the density and birefringence contours are perpendicular to the substrate temperature axis. This indicates that these material properties are determined by the substrate temperature. The symbols show the locations of individual measurements on the substrate with the colored contours interpolated from those data points.

50, 60, and 70°. This map establishes the birefringence and initial thickness of the vapor-deposited glass at each location and takes 75 min to complete. After this mapping, the as-deposited glasses are transformed into the supercooled liquid and the ordinary glass following this temperature profile: a temperature ramp to 335 K at 1 K/min, a 10 s hold at 335 K, cooling at 1 K/min to 293 K, then heating at 1 K/min to 325 K, a 10 s hold, and cooling at 1 K/min to 293 K. During the temperature ramps, ellipsometric measurements at a single incidence angle (70°) are performed sequentially on 12 locations evenly separated in space along the direction of the temperature gradient. Each of these spots is measured approximately every 4 min; this means data is collected on any given spot at intervals of about 4 K. After the temperature ramps are complete, the sample is remapped in the same

locations as the initial measurement in order to determine the final thickness and birefringence at each location. The density difference between the as-deposited material and the ordinary glass is calculated from the initial and final thicknesses. As expected, the final birefringence is zero within error (± 0.001) at each location, consistent with complete transformation into the supercooled liquid.

We estimate the error in our optical constants to be < 0.001 index units based upon control measurements of polystyrene, silicon dioxide, and the ordinary glass of indomethacin. For measurements utilizing three angles of incidence, we estimate that our error in the sample thickness is less than 0.3 nm. For samples deposited at the lowest substrate temperatures, there are indications that a wavelength-dependent birefringence term might fit the data better, but this change in the model does not influence the resulting birefringence at 632 nm. For these low substrate temperatures, the density difference between the as-deposited glass and the ordinary glass could be in error by as much as 0.2% in single-angle measurements. Only multiangle measurements are used to produce the data shown in Figures 5 and 6. During the entire sequence of ellipsometric measurements, flowing nitrogen is used to prevent water uptake of indomethacin.⁴⁸

RESULTS

High-Throughput Dilatometry. Figure 3 shows results from single-angle ellipsometry measurements, with the measurements performed at eight locations on a vapor-deposited sample of indomethacin during a single temperature ramping experiment. The sample locations correspond to the temperatures indicated. While previously each of these samples would have been individually prepared and temperature

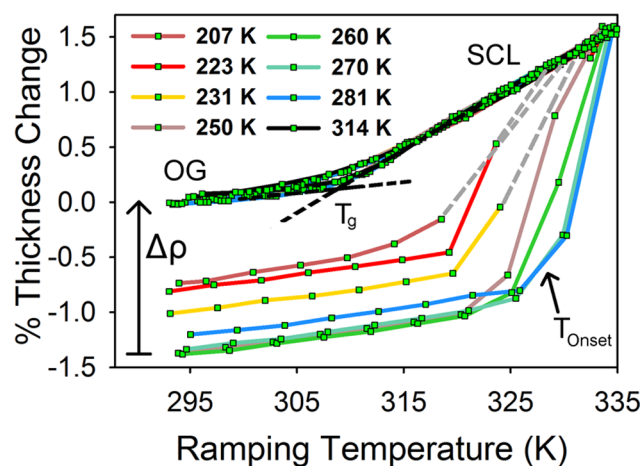


Figure 3. Evolution of the thickness of eight vapor-deposited indomethacin glasses during temperature ramping. These glasses were prepared at the indicated substrate temperatures in a single deposition (sample C), and the data shown were obtained in a single temperature ramping experiment. Each of the eight glasses initially shows a region of linear thermal expansion characteristic of an amorphous solid. The temperature T_{onset} marks the beginning of the transformation into a supercooled liquid. Beyond T_{onset} , the as-deposited lines merge to form the supercooled liquid (SCL). Cooling yields the ordinary glass (OG) with the glass transition temperature T_g indicated. Data for a second heating ramp is also shown and superposes with the data from the first cooling except near T_g . The $T_{\text{substrate}} = 314$ K data is obscured by the ordinary glasses (OG) from other substrate temperatures.

ramped over the course of about 5 days total, by utilizing the temperature gradient, these results take less than 1 day to acquire. The glasses characterized in Figure 3 represent the entire range of indomethacin glasses that are stable at room temperature.

Figure 3 illustrates two of the distinctive features of stable organic glasses. The as-deposited glasses are thinner than the ordinary glass over a large range of substrate temperatures, indicating higher density. While physically aging can increase the density of ordinary glasses, the density change that can be achieved by this approach is typically much smaller than the $\sim 1\%$ changes shown in Figure 3.^{49–52} For example, the glass vapor-deposited at $T_{\text{substrate}} = 260$ K is about 1.4% more dense than the ordinary glass. By extrapolating the supercooled liquid line in Figure 3, this corresponds to the density expected for the equilibrium supercooled liquid at 278 K. We can estimate that a liquid-cooled glass would have to be aged at or below 278 K for at least 10^3 years to achieve similar density. The second important feature shown in Figure 3 is that T_{onset} can substantially exceed T_g . This is an indication of the kinetic stability of the as-deposited glasses. T_{onset} can be increased by aging an ordinary glass, but this approach typically yields no more than a 5 K increase above the ordinary T_g ,⁵³ as opposed to the 20 K effect seen for the most stable glass in Figure 3. Once the sample is heated well beyond T_{onset} it loses all memory of its vapor-deposited state and becomes an equilibrium liquid. Further cooling and heating establish the behavior of the ordinary glass that we use as a reference state in these experiments.

While the onset temperature serves as a reasonable phenomenological characterization of the kinetic stability of a vapor-deposited glass, it does obscure the fact that stable glasses transform into the supercooled liquid by a different mechanism than does the ordinary glass. Ordinary glasses and modestly aged glasses transform into the supercooled liquid in a homogeneous fashion. In contrast, thin films⁵⁴ of stable glasses transform into the supercooled liquid via a constant velocity propagating front that initiates at the free surface.^{27,55–60} Apparently, stable glasses prepared by physical vapor deposition are so tightly packed that structural relaxation in the bulk of the sample is negligible for a thin film even 20 K above T_g . A consequence of the propagating growth front is that the sample is not optically homogeneous during the transition. Since our optical model presumes that the entire organic layer is a uniform material, the data points acquired during the transformation into the supercooled liquid are only qualitatively correct. For $T_{\text{substrate}} = 207, 223,$ and 231 K, some of these points have been removed and replaced by dashed lines to maintain clarity in Figure 3.

Figure 4 collects the onset temperatures for vapor-deposited glasses of indomethacin prepared on four temperature-gradient samples and shows for the first time the kinetic stability of glasses deposited across more than a 100 K range of substrate temperatures. Glasses with substantial kinetic stability are produced across more than a 70 K range. For materials deposited at or near the ordinary T_g (309 K), structural reorganization begins near T_g on heating, as in the liquid cooled glass. For lower substrate temperatures, states similar to the equilibrium supercooled liquid are accessed, conferring greater kinetic stability; we attribute this to enhanced surface mobility.²⁹ In this regime, kinetic stability increases with decreasing temperature. As the substrate temperature falls below 280 K, the rate of configurational sampling at the surface

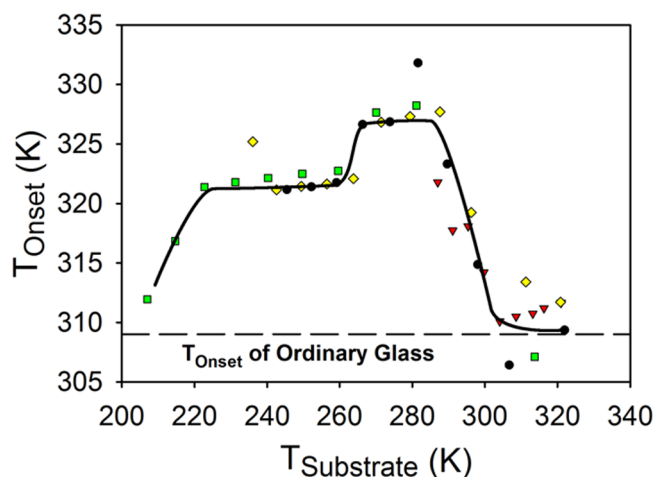


Figure 4. Kinetic stability of indomethacin glasses vapor-deposited at different substrate temperatures. T_{onset} marks the onset of structural change during temperature ramping at 1 K/min. For depositions near the glass transition temperature (309 K), T_{onset} is close to T_g . As the substrate temperature is lowered below T_g , the kinetic stability of the deposited glasses increases significantly. Data from four samples are shown; the figure legend is given in Figure 5. The line is a guide to the eye.

becomes slower than the rate of arrival of new molecules, and the resulting materials are less kinetically stable. Glasses deposited at 210 K have kinetic stability similar to that of the ordinary glass. Experiments at even lower substrate temperature (not shown here) did not yield glasses with reproducible properties; we suspect that the as-deposited glasses at these substrate temperatures are quite unstable and evolve to some extent at 293 K prior to ellipsometric measurement.

We briefly comment on some technical details regarding the data in Figure 4. For any given location on the substrate, we collect a data point at 4 K intervals during temperature scanning, and this limits our resolution in determining T_{onset} to ± 2 K. Given this lack of precision, the agreement between the different samples shown in Figure 4 is good. We report T_{onset} as the midpoint between the last temperature for which the thickness was consistent with thermal expansion of the solid and the first temperature for which this is no longer true. The previously reported²⁴ T_{onset} values for indomethacin glasses vapor-deposited under these conditions (327, 327, and 330 K at $T_{\text{substrate}}$ values of 245, 265, and 285 K, respectively) are in reasonable agreement with the values in Figure 4.

Influence of Substrate Temperature on Density. The density of the as-deposited glasses relative to the ordinary glass is determined by comparing the thickness of the sample at many locations before and after temperature ramping, as illustrated in Figure 2a and b. In Figure 5, we have compiled the density data from measurements of this type on five samples. By using the grid of measurements shown in Figure 2, we are able to capture the same density change as during temperature ramping experiments like those in Figure 3. However, the grid measurements provide higher resolution in substrate temperature because of the closer spacing of measurement points. In addition, the density values determined from the grid measurements are more accurate because ellipsometry measurements at each spot were performed at three angles of incidence.⁶¹

Figure 5 shows that indomethacin glasses deposited at $T_{\text{substrate}} > 309$ K have nearly the density of the ordinary glass.

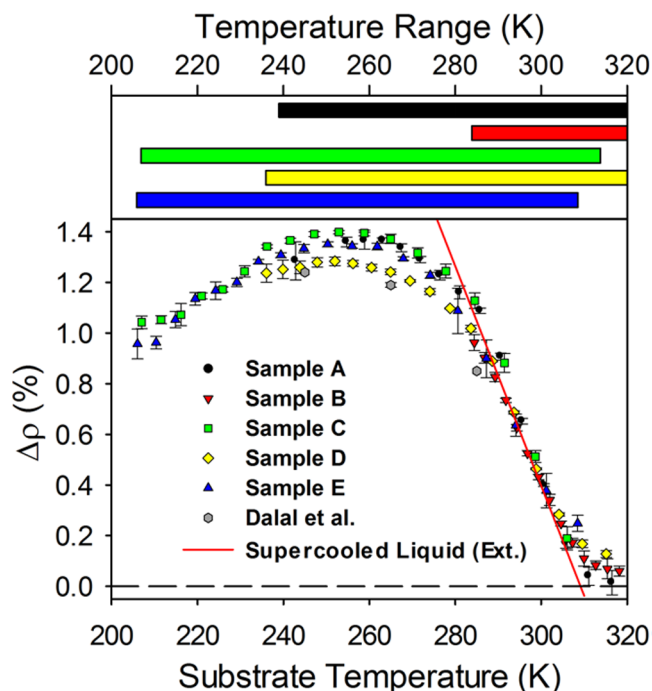


Figure 5. Density of vapor-deposited indomethacin glasses at many substrate temperatures, relative to the density of the ordinary glass. At high substrate temperatures, the density is very close to the ordinary glass, as expected. As the substrate temperature is decreased, the material prepared is denser, reaching a maximum at 255 K. The solid red line shows the density expected for the equilibrium supercooled liquid (obtained by extrapolation as explained in the text). At substrate temperatures down to 278 K, the density of the vapor-deposited glass is equal to that expected for the supercooled liquid. Each color represents an independently deposited sample; the color scheme is consistent across figures. The bars at the top show the substrate temperature range for each sample. The gray points are literature data from samples deposited at a single substrate temperature.²⁴

After the deposition is complete, we expect to have an equilibrium supercooled liquid at all of these locations on the substrate. When these liquids are cooled in the chamber, they form ordinary glasses. As the substrate temperature drops below 309 K, the density of the samples follows that of the supercooled liquid extrapolated below T_g . It is remarkable that the as-deposited glasses have the density expected for the equilibrium supercooled liquid down to 278 K. On the basis of the density measurements below $T_{\text{substrate}} = 278$ K, we infer that in this temperature regime there is insufficient mobility at the glass surface to allow the molecules to find equilibrium configurations during vapor deposition. The substrate temperature which produces materials of the highest density, 255 K, is where the competition between thermodynamic driving forces and kinetic limitations best balance to produce high density materials. As the temperature becomes lower yet, surface mobility allows little configurational sampling. We expect that, at some temperature below the range of our experiments, the as-deposited glasses would have densities even lower than the ordinary glass.

The densities shown in Figure 5 are in reasonable agreement with values reported earlier for three deposition temperatures (gray points).²⁴ The new measurements are slightly higher, by approximately 0.1%, and we attribute this to small preparation differences between samples. As shown in Figure 5, the density for samples deposited above 309 K is slightly higher than the

density of the ordinary glass. We attribute this to physical aging prior to the ellipsometry measurements. Materials deposited above T_g are cooled to 293 K where they age from 20 to 130 min before their thickness is measured. The density increase during aging can be as large as 0.07%, which reasonably explains the data in Figure 5. While this aging effect could be subtracted from the data for substrate temperatures above T_g (see the Supporting Information for data on the aging of indomethacin), we have not done so because we are unable to perform a similar correction for the as-deposited glasses prepared at lower substrate temperatures. Aging also occurs to some extent prior to the final thickness measurements, and the results are corrected for this effect.

A few details about the data in Figure 5 need to be specified. The supercooled liquid line shown in the figure is calculated from the thermal expansion coefficients previously reported for indomethacin. Because all the ellipsometry measurements are performed at 293 K, the slope of the line shown is the difference between the thermal expansion coefficient of the supercooled liquid ($5.69 \times 10^{-4}/\text{K}$) and that of the ordinary glass ($1.33 \times 10^{-4}/\text{K}$);²⁴ since the ordinary glass reference state is prepared by cooling at 1 K/min, the zero of $\Delta\rho$ is fixed to be at 309 K, the observed T_g value at this cooling rate. In Figure 5, each point has an error bar representing the 95% confidence interval for that sample at that deposition temperature, calculated by using ~ 5 measurements along the sample x -axis (see Figure 2a and b). Most of these confidence intervals are smaller than the symbol size, indicating excellent consistency between these measurements orthogonal to the temperature-gradient axis. For a few points (3 of the 90 data points acquired), the confidence intervals were greater than 0.1% and these points were excluded from the graph. We also note that sample E was transformed into the supercooled liquid by a different procedure (isothermal transformation at 325 K) than the other samples. Consistent with previous work, a correction was applied to the data for this sample, increasing the density by 0.15% to account for the observed thinning of the sample during transformation.²⁴

Influence of Substrate Temperature on Molecular Orientation. Figure 6 shows the substrate temperature dependence of the birefringence of vapor-deposited indomethacin glasses, which is indicative of the molecular orientation. At temperatures above 301 K, films are optically isotropic and have the density expected for the supercooled liquid. We anticipate that these materials are the equilibrium supercooled liquid at $T_{\text{substrate}}$. Using reasonable extrapolations of the dielectric relaxation time,⁶² we estimate that it would take at least 1 week of aging to prepare the supercooled liquid at this temperature by aging an ordinary glass. Below 301 K, the as-deposited material is no longer optically isotropic. The maximum in birefringence is at 278 K, which we interpret to indicate that the axis of indomethacin with the highest polarizability is oriented out of the plane of the substrate. As the substrate temperature drops, the birefringence passes through zero at 253 K and then becomes negative, which we interpret to mean that the high polarizability axis of indomethacin is primarily lying in the plane of the substrate.

Measurements by Yokoyama et al.^{1–4} and others have used dichroism^{9–13} (anisotropic absorption) to demonstrate that vapor-deposited organic glasses can exhibit nonrandom molecular orientations. For a number of systems, their data indicates a substantial correlation between the dichroism and the birefringence.² For molecules with strongly polarized

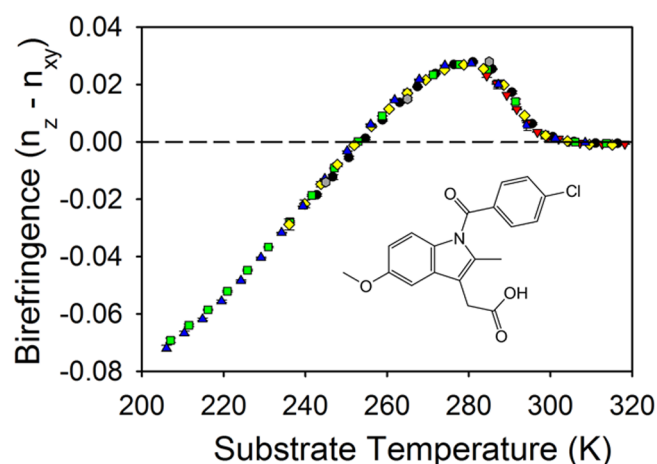


Figure 6. Birefringence of vapor-deposited indomethacin glasses as a function of substrate temperature, showing a range of molecular orientations. n_z is the index of refraction perpendicular to the substrate, and n_{xy} is the index of refraction in the plane of the substrate. Data from five samples are shown; the colors used here correspond to those used in Figure 5. The gray hexagons are previously published results for isothermal samples used as temperature calibration points in these experiments.²⁴ While this ensures that any one sample agrees with the calibration points, the excellent agreement between data sets across the temperature range argues for the accuracy of the temperature for all measurements. Error bars indicate 95% confidence intervals. The inset shows the molecular structure of indomethacin.

transitions, dichroism provides a more straightforward connection to molecular orientation. Dichroism can be extracted from ellipsometry measurements which fit data in the wavelength range of the absorption. In future work, we will use dichroism to better characterize molecular orientation for glasses prepared on substrates with temperature gradients.

DISCUSSION

We separate the information that we are able to obtain from experiments on vapor-deposited indomethacin glasses into two categories. We first compare two properties that provide information about the anisotropy of the local packing environment. We then compare three different macroscopic material properties. In the discussion that follows, we use these comparisons to divide vapor-deposited glasses into three regimes of substrate temperature.

Comparison of Measures of Anisotropic Local Packing in Vapor-Deposited Glasses. Two probes of anisotropic local packing in vapor-deposited indomethacin glasses, the birefringence and the anisotropic scattering in WAXS, are compared in Figure 7a. The birefringence is a measure of molecular orientation, as discussed above. WAXS experiments on vapor-deposited indomethacin show an anisotropic peak at low wavevector that is not present in the supercooled liquid or ordinary glass.⁴⁸ The intensity of this peak is shown in Figure 7a for three different deposition rates. The anisotropic WAXS peak indicates that the electron density is modulated in the direction perpendicular to the sample surface with a roughly 1 nm period (approximately the diameter of an indomethacin molecule) and a ~ 3 nm coherence length. This could indicate a tendency toward molecular layering, as indicated in computer simulations of vapor deposited glasses.²⁶ The figure portrays the relative WAXS peak intensities for all the indomethacin samples, and

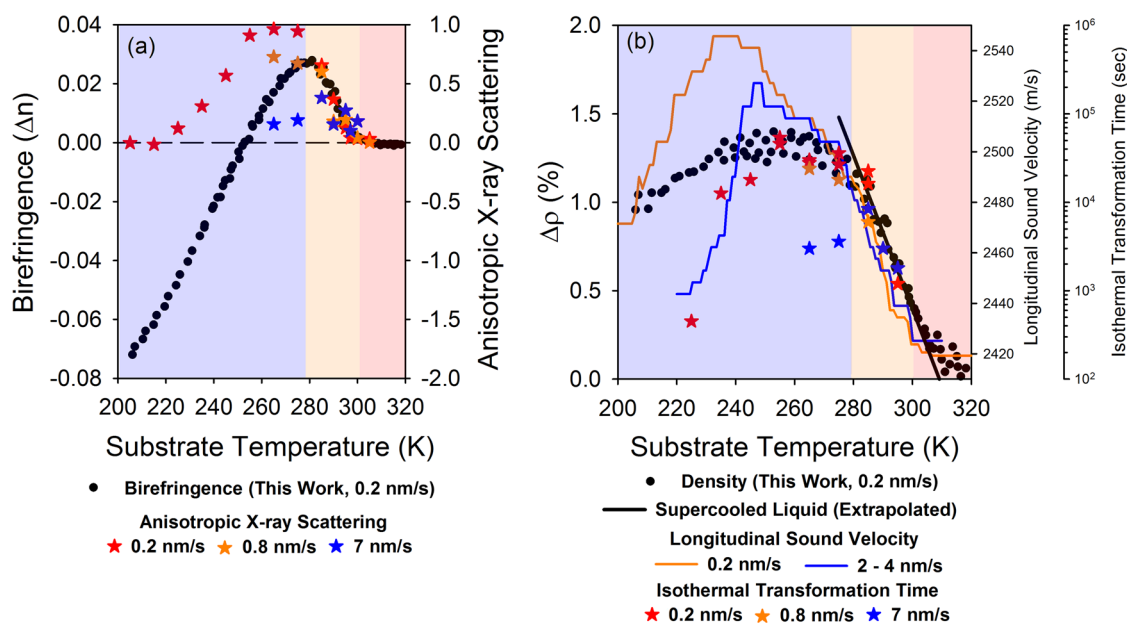


Figure 7. Comparison of observables for vapor-deposited indomethacin glasses, interpreted in terms of three substrate temperature regimes. At the highest substrate temperatures, vapor-deposited materials are apparently in equilibrium. At intermediate substrate temperatures, the vapor-deposited glasses show macroscopic signatures of equilibration but local packing is anisotropic. At the lowest substrate temperatures, the macroscopic observables become uncorrelated due to the strong influence of kinetics. (a) The anisotropy of the local packing environment is characterized by birefringence and previously published wide-angle X-ray scattering (WAXS).⁴⁸ (b) Macroscopic properties are represented by the density and previously published results for the speed of sound⁴⁵ and the isothermal transformation time.⁴⁸

we chose to scale the WAXS data to the birefringence data so that there is good overlap at high temperatures for depositions at 0.2 nm/s.

The combined birefringence and WAXS data indicate that isotropic materials are prepared at temperatures above 301 K. As discussed below, we expect that these as-deposited materials are the equilibrium supercooled liquid at the substrate temperature. At somewhat lower temperatures, both experiments indicate anisotropy, but it appears that the two observables are largely uncorrelated. At the lowest substrate temperatures, the WAXS data are consistent with an isotropic material, while the birefringence is clearly not consistent with such a view.

We do not have enough information to uniquely interpret the combined birefringence and WAXS data in molecular terms. While a plausible packing arrangement consistent with these observables is clearly desirable and would, for example, be very useful for understanding charge mobility in similar vapor-deposited glasses, this information is not required for describing the three temperature regimes for vapor-deposition that we discuss below. We anticipate that molecular simulations will be required for further progress in understanding the molecular packing. The data in Figure 7a leads to some interesting questions: Assuming that the packing measured in the bulk is achieved by molecules very near the surface during deposition, why does the surface at different temperatures cause molecules to adopt different orientations (“standing up” vs “lying down”)? Are there two states of molecular orientation that are mixed to produce intermediate values of the birefringence, or does the local orientation evolve continuously? Future experimental work will establish the extent to which the features shown in Figure 7a are observed for other molecules.

Comparison of Macroscopic Properties of Vapor-Deposited Glasses. In Figure 7b, we compare three macroscopic properties of vapor-deposited indomethacin

glasses. The density data is from this work and is described above. The longitudinal sound velocity was determined by Brillouin light scattering using deposition onto a substrate with a temperature gradient, with values for two different deposition rates shown; this data has been smoothed and is represented by the running median.⁴⁵ The longitudinal sound velocity is directly related to the longitudinal modulus such that larger sound velocities indicate mechanically stiffer glasses. The third property plotted in Figure 7b is the isothermal transformation time for thick stable glasses (25 μm), as determined by the disappearance of the anisotropic WAXS peak.⁴⁸ This transformation time is a measure of the kinetic stability of the vapor-deposited glass. For this observable, all transformations were performed at 319 K and data is shown for three different deposition rates. The y-axes for the first two observables are chosen so that they share the same extrapolated supercooled liquid line. The y-axis for the transformation time is chosen such that the data between 280 and 295 K matches the supercooled liquid line.

Three Temperature Regimes for Vapor-Deposited Glasses. On the basis of Figure 7, we separate the behavior of vapor-deposited indomethacin into three phenomenological temperature regimes that are color-coded in the figure. The high temperature regime is composed of vapor-deposited states that are in thermodynamic equilibrium (excluding the crystalline state); i.e., our experiments cannot distinguish these materials from the equilibrium supercooled liquid at $T_{\text{substrate}}$. In the intermediate temperature regime, quasi-equilibrium states are prepared which have the bulk properties expected for the equilibrium supercooled liquid while having local structures which are anisotropic and thus not strictly compatible with the supercooled liquid. In the low temperature regime, the glasses are prepared in a kinetically controlled regime and have properties that are essentially unconnected to those expected at equilibrium. While the high and low

temperature regimes are elaborations of earlier ideas, evidence for an intermediate temperature regime is presented here for the first time.

Equilibrium States. The experimental evidence is consistent with the view that deposition above 301 K prepares materials in thermodynamic equilibrium. There is no evidence of anisotropy in the materials deposited in this regime. Samples deposited above 309 K (T_g), when cooled to room temperature after deposition, have the properties expected for the ordinary glass. Samples deposited between 301 and 309 K have the properties expected for the equilibrium supercooled liquids at these temperatures, as shown in Figure 7b. We interpret this to mean that mobility at the surface of the growing glass during deposition is sufficient to allow complete equilibration. For this reason, the density, sound velocity, and isothermal transformation time are well correlated in this high temperature regime.

Quasi-Equilibrium States. In the range of substrate temperatures from 278 to 301 K, if we considered only the macroscopic properties shown in Figure 7b, we would conclude that the vapor-deposited glasses are in thermodynamic equilibrium. In this temperature regime, materials deposited at different rates have the same macroscopic properties, and these properties match what is expected for the supercooled liquid by extrapolation. This is consistent with the idea that surface mobility during these depositions is large enough to allow complete equilibration in the surface layer as the deposition continues. On the other hand, if we consider the measures of local anisotropic packing shown in Figure 7a, we would conclude that none of the vapor-deposited glasses in this temperature range are at equilibrium because they are all anisotropic. (We are not aware of any data suggesting indomethacin forms a liquid crystal, and thus, we assume that the relevant thermodynamic equilibrium state is an isotropic liquid.) That anisotropy might be present is not surprising given the inherently anisotropic nature of the vapor-deposition process, but it is surprising that this anisotropy coexists with apparently equilibrium macroscopic properties.

We describe glasses that combine anisotropy and apparently equilibrium macroscopic properties as “quasi-equilibrium” states. One way to understand this combination is to assume that the degree of anisotropic packing is small. In this case, the local packing might not be perturbed sufficiently to modify the density, sound velocity, or transformation time. This would allow the equilibrium-like correlations between macroscopic properties that are shown in Figure 7b. One further correlation is shown in Figure 8, using data collected above 278 K from the temperature gradient samples prepared for this study. A strong correlation is shown between T_{onset} and the density for glasses deposited above 278 K. We expect both density and T_{onset} to increase as a system is equilibrated lower in the potential energy landscape, and this expectation is followed in the quasi-equilibrium regime. In the lowest temperature regime, below 278 K, the correlation between density and T_{onset} is weaker (not shown).

This hypothesis about the quasi-equilibrium temperature regime could be tested in at least two ways. If temperature-gradient experiments are performed with molecules that form more highly anisotropic glasses, we expect that the temperature window of this regime will narrow, since the macroscopic properties should be more strongly influenced by the anisotropic packing. For materials like indomethacin, studies at lower deposition rates would be useful. For example, if the

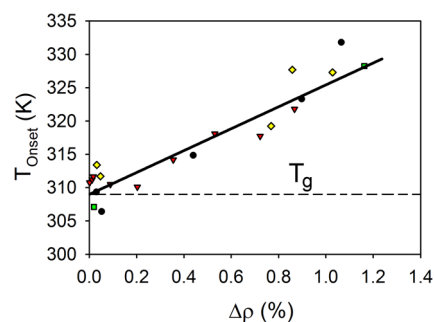


Figure 8. Onset temperature as a function of glass density for indomethacin vapor-deposited at substrate temperatures above 278 K. The glass density is presented as the fractional increase above the ordinary glass density. In this temperature range, an excellent correlation is observed between T_{onset} and density. While such a correlation is expected for equilibrium states, the data shown includes both equilibrium and quasi-equilibrium states. The line through the data is a guide to the eye. Different samples are identified by color, consistent with Figure 5.

as-deposited glass density tracked the extrapolated supercooled liquid line down to even lower substrate temperatures, that would be consistent with this hypothesis. Whether such glasses, which in terms of macroscopic properties would be nearer to equilibrium, would also be more nearly isotropic is not clear. Existing evidence from WAXS argues against this, as shown in Figure 7a.

Kinetically Controlled States. Physical vapor deposition of several organic molecules has shown that optimal stability is produced by deposition onto substrates near $0.85 T_g$. This has been explained as a competition between kinetic control and thermodynamic control. Very near T_g , mobility is high enough to allow equilibrium configurations to be achieved during deposition, but in this regime, equilibrated systems are only a little more stable than ordinary glasses. At very low temperatures, mobility at the surface is so low that the system has no opportunity to utilize the large thermodynamic driving force for equilibration and thus little stability is expected.³⁰ At some optimal, intermediate deposition temperature, significant stability is observed because surface mobility is high enough to take advantage of the substantial thermodynamic driving force for moving lower in the energy landscape.

According to this view, near the substrate temperature that produces the most stable glasses, glass formation is kinetically influenced to a significant extent. For the present discussion, we consider all glasses produced below 278 K to be “kinetically controlled.” The states in the potential energy landscape that are populated in this regime do not need to have any relationship to equilibrium states or to the non-equilibrium states that are visited during the aging of an ordinary glass. Because of this, correlations that exist among different observables in equilibrium or during physical aging need not be respected. The point is clearly illustrated in Figure 7b. Below 278 K, each observable has its own trend in relation to substrate temperature. Furthermore, in this regime, observables that were independent of deposition rate at high temperature become dependent on deposition rate. Glasses in this regime can show combinations of properties that cannot be understood or predicted on the basis of the behavior of equilibrium states. For example, deposition near 220 K at 0.2 nm/s produces a glass with a very high speed of sound (and correspondingly high

mechanical moduli) whose kinetic stability is only slightly higher than the ordinary glass.

While the kinetically controlled regime is the most difficult to understand, it likely produces the most interesting materials as density, modulus, and kinetic stability are all maximized in this regime. In addition, the temperature window between 230 and 278 K produces glasses of high kinetic stability in which molecular orientation can be systematically tuned through an interesting range, as indicated by the change in sign of the birefringence.

Work by others on model glass formers has produced vapor-deposited materials with densities as much as 10% lower than the equilibrium supercooled liquid for $T_{\text{substrate}}$ near 0.6–0.7 T_g ,^{63,64} and up to 2% higher than the equilibrium supercooled liquid for $T_{\text{substrate}}$ near 0.95 T_g . By comparison, the range of densities that we report for indomethacin glasses is much smaller and the density never exceeds that expected for the supercooled liquid. These observations deserve further investigation.

CONCLUSIONS

A method for the high-throughput preparation and characterization of vapor-deposited organic glasses has been presented. Depositing directly onto a substrate with a large temperature gradient allows many different glasses to be prepared simultaneously. Ellipsometry provides an efficient means of characterizing these glasses, allowing the determination of density, birefringence, and kinetic stability as a function of substrate temperature.

For vapor-deposited indomethacin glasses, the influence of the substrate temperature can be described in three different regimes. At the highest deposition temperatures (down to about $T_g - 8$ K), the deposited materials have the properties expected for the equilibrium supercooled liquid and are isotropic. In the intermediate temperature regime (down to $T_g - 31$ K), anisotropic materials are prepared that have the macroscopic properties of the equilibrium supercooled liquid. In the lowest temperature regime, the properties of the vapor-deposited glasses are strongly influenced by kinetic factors. Various macroscopic properties are no longer correlated with each other in this regime, allowing unusual combinations of properties. Anisotropic glasses are also produced in this low temperature regime, including systems with an interesting range of molecular orientations.

The high-throughput characterization scheme described here could be used to understand how molecular shape and functionality influence the types of glasses that can be produced by vapor deposition. It can also be used to efficiently characterize molecules of interest for particular applications, such as organic electronics. An important aspect of our future work with this method will be the addition of dichroism measurements, as these produce more direct information about molecular orientation than can be acquired from the birefringence. We are optimistic that the detailed characterization provided by the temperature gradient stage will enable computer simulations to provide a full description of the packing in vapor-deposited glasses.

ASSOCIATED CONTENT

Supporting Information

Representative data for the index of refraction of vapor-deposited indomethacin and the aging rate of indomethacin.

This material is available free of charge via the Internet at <http://pubs.acs.org>.

AUTHOR INFORMATION

Corresponding Author

*E-mail: ediger@chem.wisc.edu.

Notes

The authors declare no competing financial interest.

ACKNOWLEDGMENTS

We gratefully acknowledge the help of Rick Pfeifer and Kendall Schneider of the University of Wisconsin—Madison Department of Chemistry Instrument Shop in the construction of the temperature gradient stage. We thank Mikhail Yu. Efremov for discussions regarding thermal contact. This work was funded by the U.S. Department of Energy, Office of Basic Energy Sciences, Division of Materials Sciences and Engineering, award DE-SC0002161.

REFERENCES

- (1) Yokoyama, D.; Nakayama, K.; Otani, T.; Kido, J. Wide-Range Refractive Index Control of Organic Semiconductor Films toward Advanced Optical Design of Organic Optoelectronic Devices. *Adv. Mater.* **2012**, *24*, 6368–6373.
- (2) Yokoyama, D. Molecular Orientation in Small-Molecule Organic Light-Emitting Diodes. *J. Mater. Chem.* **2011**, *21*, 19187.
- (3) Yokoyama, D.; Sakaguchi, A.; Suzuki, M.; Adachi, C. Horizontal Molecular Orientation in Vacuum-Deposited Organic Amorphous Films of Hole and Electron Transport Materials. *Appl. Phys. Lett.* **2008**, *93*, 173302.
- (4) Yokoyama, D.; Sakaguchi, A.; Suzuki, M.; Adachi, C. Horizontal Orientation of Linear-Shaped Organic Molecules Having Bulky Substituents in Neat and Doped Vacuum-Deposited Amorphous Films. *Org. Electron.* **2009**, *10*, 127–137.
- (5) Yokoyama, D.; Setoguchi, Y.; Sakaguchi, A.; Suzuki, M.; Adachi, C. Orientation Control of Linear-Shaped Molecules in Vacuum-Deposited Organic Amorphous Films and Its Effect on Carrier Mobilities. *Adv. Funct. Mater.* **2010**, *20*, 386–391.
- (6) Yokoyama, D.; Adachi, C. In Situ Real-Time Spectroscopic Ellipsometry Measurement for the Investigation of Molecular Orientation in Organic Amorphous Multilayer Structures. *J. Appl. Phys.* **2010**, *107*, 123512.
- (7) Kim, J. Y.; Yokoyama, D.; Adachi, C. Horizontal Orientation of Disk-Like Hole Transport Molecules and Their Application for Organic Light-Emitting Diodes Requiring a Lower Driving Voltage. *J. Phys. Chem. C* **2012**, *116*, 8699–8706.
- (8) Debe, M. K. Variable Angle Spectroscopic Ellipsometry Studies of Oriented Phthalocyanine Films. *J. Vac. Sci. Technol., A* **1991**, *9*, 1265.
- (9) Debe, M. K. Variable Angle Spectroscopic Ellipsometry Studies of Oriented Phthalocyanine Films. II. Copper Phthalocyanine. *J. Vac. Sci. Technol., A* **1992**, *10*, 2816.
- (10) Egelhaaf, H.-J.; Gierschner, J.; Haiber, J.; Oelkrug, D. Optical Constants of Highly Oriented Oligothiophene Films and Nanoparticles. *Opt. Mater.* **1999**, *12*, 395–401.
- (11) Oelkrug, D.; Egelhaaf, H.-J.; Haiber, J. Electronic Spectra of Self-Organized Oligothiophene Films with “Standing” and “Lying” Molecular Units. *Thin Solid Films* **1996**, *284–285*, 267–270.
- (12) Oh-e, M.; Ogata, H.; Fujita, Y.; Koden, M. Anisotropy in Amorphous Films of Cross-Shaped Molecules with an Accompanying Effect on Carrier Mobility: Ellipsometric and Sum-Frequency Vibrational Spectroscopic Studies. *Appl. Phys. Lett.* **2013**, *102*, 101905.
- (13) Schuenemann, C.; Petrich, A.; Schulze, R.; Wynands, D.; Meiss, J.; Hein, M. P.; Jankowski, J.; Elschner, C.; Alex, J.; Hummert, M.; et al. Diindenoperylene Derivatives: A Model to Investigate the Path from Molecular Structure via Morphology to Solar Cell Performance. *Org. Elec.* **2013**, *14*, 1704–1714.

- (14) Lin, H. W.; Lin, C. L.; Chang, H. H.; Lin, Y. T.; Wu, C. C.; Chen, Y. M.; Chen, R. T.; Chien, Y. Y.; Wong, K. T. Anisotropic Optical Properties and Molecular Orientation in Vacuum-Deposited Ter(9,9-diarylfuorene)s Thin Films Using Spectroscopic Ellipsometry. *J. Appl. Phys.* **2004**, *95*, 881–886.
- (15) Lin, H.-W.; Lin, C.-L.; Wu, C.-C.; Chao, T.-C.; Wong, K.-T. Influences of Molecular Orientations on Stimulated Emission Characteristics of Oligofluorene Films. *Org. Elec.* **2007**, *8*, 189–197.
- (16) Farahzadi, A.; Beigmohamadi, M.; Niyamakom, P.; Kremers, S.; Meyer, N.; Heuken, M.; Wuttig, M. Characterization of Amorphous Organic Thin Films, Determination of Precise Model for Spectroscopic Ellipsometry Measurements. *Appl. Surf. Sci.* **2010**, *256*, 6612–6617.
- (17) Frischeisen, J.; Yokoyama, D.; Endo, A.; Adachi, C.; Brütting, W. Increased Light Outcoupling Efficiency in Dye-Doped Small Molecule Organic Light-Emitting Diodes with Horizontally Oriented Emitters. *Org. Electron.* **2011**, *12*, 809–817.
- (18) Swallen, S. F.; Kearns, K. L.; Mapes, M. K.; Kim, Y. S.; McMahon, R. J.; Ediger, M. D.; Wu, T.; Yu, L.; Satija, S. Organic Glasses with Exceptional Thermodynamic and Kinetic Stability. *Science* **2007**, *315*, 353–356.
- (19) Leon-Gutierrez, E.; Sepúlveda, A.; Garcia, G.; Clavaguera-Mora, M. T.; Rodríguez-Viejo, J. Stability of Thin Film Glasses of Toluene and Ethylbenzene Formed by Vapor Deposition: An in Situ Nanocalorimetric Study. *Phys. Chem. Chem. Phys.* **2010**, *12*, 14693.
- (20) Leon-Gutierrez, E.; Garcia, G.; Lopeandia, A. F.; Clavaguera-Mora, M. T.; Rodríguez-Viejo, J. Size Effects and Extraordinary Stability of Ultrathin Vapor Deposited Glassy Films of Toluene. *J. Phys. Chem. Lett.* **2010**, *1*, 341–345.
- (21) León-Gutiérrez, E.; Garcia, G.; Clavaguera-Mora, M. T.; Rodríguez-Viejo, J. Glass Transition in Vapor Deposited Thin Films of Toluene. *Thermochim. Acta* **2009**, *492*, 51–54.
- (22) Swallen, S. F.; Kearns, K. L.; Satija, S.; Traynor, K.; McMahon, R. J.; Ediger, M. D. Molecular View of the Isothermal Transformation of a Stable Glass to a Liquid. *J. Chem. Phys.* **2008**, *128*, 214514.
- (23) Dalal, S. S.; Sepúlveda, A.; Pribil, G. K.; Fakhraai, Z.; Ediger, M. D. Density and Birefringence of a Highly Stable α,α,β -trisnaphthylbenzene Glass. *J. Chem. Phys.* **2012**, *136*, 204501.
- (24) Dalal, S. S.; Ediger, M. D. Molecular Orientation in Stable Glasses of Indomethacin. *J. Phys. Chem. Lett.* **2012**, *3*, 1229–1233.
- (25) Kearns, K. L.; Swallen, S. F.; Ediger, M. D.; Wu, T.; Sun, Y.; Yu, L. Hiking down the Energy Landscape: Progress toward the Kauzmann Temperature via Vapor Deposition. *J. Phys. Chem. B* **2008**, *112*, 4934–4942.
- (26) Singh, S.; de Pablo, J. J. A Molecular View of Vapor Deposited Glasses. *J. Chem. Phys.* **2011**, *134*, 194903.
- (27) Leonard, S.; Harrowell, P. Macroscopic Facilitation of Glassy Relaxation Kinetics: Ultrastable Glass Films with Frontlike Thermal Response. *J. Chem. Phys.* **2010**, *133*, 244502.
- (28) Ramos, S. L. L. M.; Oguni, M.; Ishii, K.; Nakayama, H. Character of Devitrification, Viewed from Enthalpic Paths, of the Vapor-Deposited Ethylbenzene Glasses. *J. Phys. Chem. B* **2011**, *115*, 14327–14332.
- (29) Zhu, L.; Brian, C. W.; Swallen, S. F.; Straus, P. T.; Ediger, M. D.; Yu, L. Surface Self-Diffusion of an Organic Glass. *Phys. Rev. Lett.* **2011**, *106*, 256103.
- (30) Takeda, K.; Yamamuro, O.; Oguni, M.; Suga, H. Calorimetric Study on Structural Relaxation of 1-Pentene in Vapor-Deposited and Liquid-Quenched Glassy States. *J. Phys. Chem.* **1995**, *99*, 1602–1607.
- (31) Ishii, K.; Nakayama, H.; Moriyama, R. Nonequilibrium and Relaxation in Deeply Supercooled Liquid of Isopropylbenzene Obtained through Glass Transition from Vapor-Deposited Glass. *J. Phys. Chem. B* **2012**, *116*, 935–942.
- (32) Ediger, M. D.; Angell, C. A.; Nagel, S. R. Supercooled Liquids and Glasses. *J. Phys. Chem.* **1996**, *100*, 13200–13212.
- (33) Ediger, M. D.; Harrowell, P. Perspective: Supercooled Liquids and Glasses. *J. Chem. Phys.* **2012**, *137*, 080901.
- (34) Debenedetti, P. G.; Stillinger, F. H. Supercooled Liquids and the Glass Transition. *Nature* **2001**, *410*, 259.
- (35) Heuer, A. Exploring the Potential Energy Landscape of Glass-Forming Systems: From Inherent Structures via Metabasins to Macroscopic Transport. *J. Phys.: Condens. Matter* **2008**, *20*, 373101.
- (36) Komiya, S. Physical Vapor Deposition of Thick Cr and Its Carbide and Nitride Films by Hollow-Cathode Discharge. *J. Vac. Sci. Technol.* **1976**, *13*, 520.
- (37) Chikyow, T.; Ahmet, P.; Nakajima, K.; Koida, T.; Takakura, M.; Yoshimoto, M.; Koinuma, H. A Combinatorial Approach in Oxide/Semiconductor Interface Research for Future Electronic Devices. *Appl. Surf. Sci.* **2002**, *189*, 284–291.
- (38) Jehn, H. A. Morphology and Properties of Sputtered (Ti,Al)N Layers on High Speed Steel Substrates as a Function of Deposition Temperature and Sputtering Atmosphere. *J. Vac. Sci. Technol., A* **1986**, *4*, 2701.
- (39) Christen, H. M.; Jellison, G. E.; Ohkubo, I.; Huang, S.; Reeves, M. E.; Cicerella, E.; Freeouf, J. L.; Jia, Y.; Schlom, D. G. Dielectric and Optical Properties of Epitaxial Rare-Earth Scandate Films and Their Crystallization Behavior. *Appl. Phys. Lett.* **2006**, *88*, 262906.
- (40) Christen, H. M.; Eres, G. Recent Advances in Pulsed-Laser Deposition of Complex Oxides. *J. Phys.: Condens. Matter* **2008**, *20*, 264005.
- (41) Baldo, M. A.; Kozlov, V. G.; Burrows, P. E.; Forrest, S. R.; Ban, V. S.; Koene, B.; Thompson, M. E. Low Pressure Organic Vapor Phase Deposition of Small Molecular Weight Organic Light Emitting Device Structures. *Appl. Phys. Lett.* **1997**, *71*, 3033–3035.
- (42) Bauer, S.; Stock, N. Implementation of a Temperature-Gradient Reactor System for High-Throughput Investigation of Phosphonate-Based Inorganic–Organic Hybrid Compounds. *Angew. Chem., Int. Ed.* **2007**, *119*, 6981–6984.
- (43) Meredith, J. C.; Smith, A. P.; Karim, A.; Amis, E. J. Combinatorial Materials Science for Polymer Thin-Film Dewetting. *Macromolecules* **2000**, *33*, 9747–9756.
- (44) Meyer, R.; Hamann, S.; Ehmann, M.; Thienhaus, S.; Jaeger, S.; Thiede, T.; Devi, A.; Fischer, R. A.; Ludwig, A. Microgradient-Heaters as Tools for High-Throughput Experimentation. *ACS Comb. Sci.* **2012**, *14*, 531–536.
- (45) Fakhraai, Z.; Still, T.; Fytas, G.; Ediger, M. D. Structural Variations of an Organic Glassformer Vapor-Deposited onto a Temperature Gradient Stage. *J. Phys. Chem. Lett.* **2011**, *2*, 423–427.
- (46) Yaws, C. L. *Transport Properties of Chemicals and Hydrocarbons*; Electronic: Norwich, NY, 2010.
- (47) *Mathematica*, version 8; Wolfram Research, Inc.: Champaign, IL, 2010.
- (48) Dawson, K. J.; Zhu, L.; Yu, L.; Ediger, M. D. Anisotropic Structure and Transformation Kinetics of Vapor-Deposited Indomethacin Glasses. *J. Phys. Chem. B* **2011**, *115*, 455–463.
- (49) Baker, E. A.; Rittigstein, P.; Torkelson, J. M.; Roth, C. B. Streamlined Ellipsometry Procedure for Characterizing Physical Aging Rates of Thin Polymer Films. *J. Polym. Sci., Part B: Polym. Phys.* **2009**, *47*, 2509–2519.
- (50) Robertson, C. G.; Wilkes, G. L. Refractive Index: A Probe for Monitoring Volume Relaxation During Physical Aging of Glassy Polymers. *Polymer* **1998**, *39*, 2129–2133.
- (51) Simon, S. L.; Sobieski, J. W.; Plazek, D. J. Volume and Enthalpy Recovery of Polystyrene. *Polymer* **2001**, *42*, 2555–2567.
- (52) Huang, Y.; Paul, D. R. Physical Aging of Thin Glassy Polymer Films Monitored by Optical Properties. *Macromolecules* **2006**, *39*, 1554–1559.
- (53) Vyazovkin, S.; Dranca, I. Effect of Physical Aging on Nucleation of Amorphous Indomethacin. *J. Phys. Chem. B* **2007**, *111*, 7283–7287.
- (54) Kearns, K. L.; Ediger, M. D.; Huth, H.; Schick, C. One Micrometer Length Scale Controls Kinetic Stability of Low-Energy Glasses. *J. Phys. Chem. Lett.* **2010**, *1*, 388–392.
- (55) Swallen, S. F.; Traynor, K.; McMahon, R. J.; Ediger, M. D. Stable Glass Transformation to Supercooled Liquid via Surface-Initiated Growth Front. *Phys. Rev. Lett.* **2009**, *102*, 65503.
- (56) Sepúlveda, A.; Leon-Gutierrez, E.; Gonzalez-Silveira, M.; Clavaguera-Mora, M. T.; Rodríguez-Viejo, J. Anomalous Transformation of Vapor-Deposited Highly Stable Glasses of Toluene into

Mixed Glassy States by Annealing Above T_g . *J. Phys. Chem. Lett.* **2012**, *3*, 919–923.

(57) Sepúlveda, A.; Swallen, S. F.; Kopff, L. A.; McMahon, R. J.; Ediger, M. D. Stable Glasses of Indomethacin and α,α,β -trinitrophenylbenzene Transform into Ordinary Supercooled Liquids. *J. Chem. Phys.* **2012**, *137*, 204508.

(58) Sepúlveda, A.; Swallen, S. F.; Ediger, M. D. Manipulating the Properties of Stable Organic Glasses Using Kinetic Facilitation. *J. Chem. Phys.* **2013**, *138*, 12A517.

(59) Komino, T.; Nomura, H.; Yahiro, M.; Adachi, C. Real-Time Measurement of Molecular Orientational Randomization Dynamics During Annealing Treatments by In-Situ Ellipsometry. *J. Phys. Chem. C* **2012**, *116*, 11584–11588.

(60) Wolynes, P. G. Spatiotemporal Structures in Aging and Rejuvenating Glasses. *Proc. Natl. Acad. Sci. U.S.A.* **2009**, *106*, 1353–1358.

(61) Woollam, J. A.; Johs, B.; Herzinger, C.; Hilfiker, J.; Synowicki, R.; Bungay, C. Overview of Variable Angle Spectroscopic Ellipsometry (VASE), Part I: Basic Theory of Typical Applications. *SPIE Proc.* **1999**, *CR72*, 3–28.

(62) Wojnarowska, Z.; Adrjanowicz, K.; Włodarczyk, P.; Kaminska, E.; Kaminski, K.; Grzybowska, K.; Wrzalik, R.; Paluch, M.; Ngai, K. L. Broadband Dielectric Relaxation Study at Ambient and Elevated Pressure of Molecular Dynamics of Pharmaceutical: Indomethacin. *J. Phys. Chem. B* **2009**, *113*, 12536–12545.

(63) Ishii, K.; Nakayama, H.; Hirabayashi, S.; Moriyama, R. Anomalous High-Density Glass of Ethylbenzene Prepared by Vapor Deposition at Temperatures Close to the Glass-Transition Temperature. *Chem. Phys. Lett.* **2008**, *459*, 109–112.

(64) Ishii, K.; Nakayama, H.; Moriyama, R.; Yokoyama, Y. Behavior of Glass and Supercooled Liquid Alkylbenzenes Vapor-Deposited on Cold Substrates: Toward the Understanding of the Curious Light Scattering Observed in Some Supercooled Liquid States. *Bull. Chem. Soc. Jpn.* **2009**, *82*, 1240–1247.

■ NOTE ADDED AFTER ASAP PUBLICATION

This paper was published ASAP on August 8, 2013. The size of Figure 5 has been increased. The corrected version was reposted on August 23, 2013.